

1 A long look at short prokaryotic Argonautes

2 Balwina Koopal¹, Sumanth K. Mutte¹, Daan C. Swarts^{1,*}

3 ¹Laboratory of Biochemistry, Wageningen University, 6708 WE, Wageningen, The Netherlands

4 *Lead contact (daan.swarts@wur.nl)

5 Abstract

6 Argonaute proteins (Agos) use small 15-30 nucleotide-long guides to bind and/or cleave complementary target nucleic
7 acids. Eukaryotic Agos mediate RNA-guided RNA silencing, while 'long' prokaryotic Agos (pAgos) use RNA or DNA guides
8 to interfere with invading plasmid and viral DNA. Here, we review the function and mechanisms of truncated and highly
9 divergent 'short' pAgos, which, until recently, remained functionally uncharacterized. Short pAgos retained the MID and
10 PIWI domains important for guide-mediated target binding, but lack the ability to cleave their targets. Instead, emerging
11 insights reveal that various short pAgos interact with distinct accessory 'effector' enzymes. Upon guide-mediated detection
12 of invading DNA by short pAgos, their associated effector enzymes kill the host cell and consequentially prevent spread
13 of the invader.

14 Keywords

15 Prokaryotic Argonaute (pAgo), host defense, short pAgo, prokaryotic immunity, host defense, abortive infection

16 Argonaute proteins are found in all domains of life

17 In all domains of life, Argonaute proteins (Agos) use small (15-30 nucleotides) oligonucleotides as guides to bind
18 complementary nucleic acid targets. Eukaryotic Argonautes (eAgos) are the key effector enzymes in RNA silencing
19 pathways and can be subdivided in two main clades: eAGO and ePIWI (lineage-specific eAgos are not discussed here).
20 eAGOs generally bind small interfering RNA (siRNA) or microRNA (miRNA) guides generated by Dicer and/or Drosha
21 nucleases [1]. Together with accessory proteins, eAGO forms an RNA-induced silencing complex (RISC) that silences
22 mRNA targets to regulate gene expression [1]. ePIWIs bind PIWI-interacting RNA (piRNA) guides generated from longer
23 genomic transcripts [2]. ePIWIs mainly silence transposons by cleaving their transcripts or by recruiting accessory proteins
24 that induce heterochromatin formation [2-4].

25 Compared to eAgos, prokaryotic Argonaute proteins (pAgos) are highly diversified in sequence and domain composition
26 [5-7]. They show a patchy distribution over the bacterial and archaeal phyla [5] and are often associated with other host
27 defense genes in so called "defense islands": clusters of genes related to prokaryotic defense [7,8]. Based on their genetic
28 association with other defense genes, their (predicted) nuclease activity, and because they are frequently subjected to
29 horizontal gene transfer, it was hypothesized that pAgos play a role in host defense against invading DNA such as plasmids
30 and viruses [7]. Based on their phylogeny, pAgos can be subdivided in long-A, long-B, and short pAgos (Figure 1A). Long-
31 A and long-B pAgos have a canonical bilobed N-PAZ-MID-PIWI domain composition like eAgos [9-12] (Figures 1 and 2A-
32 C; Box 1). While this suggests that Agos in all domains of life rely on similar mechanisms, proteins that are typically
33 required in eukaryotic RNA silencing pathways (e.g. Dicer), have not been identified in prokaryotes [13]. Therefore, it is
34 likely that pAgos execute different functions. In contrast, short pAgos lack the N- and PAZ domains, and are thus comprised
35 of the MID and PIWI domains only (Figures 1 and 2D-I).

36 79% of the long-A pAgos have an intact catalytic DEDX tetrad (Box 1) in the PIWI domain, and most characterized long-
37 A pAgos are capable of DNA guide-mediated target DNA cleavage [12,14-18][12,14-18]. However, at least *in vitro*, one

38 long-A pAgo uses RNA guides to target DNA [19], others use DNA guides to target RNA [20,21], and some do not have
39 a clear preference for a specific type of guide and target [22,23]. In accordance with earlier hypotheses [7], catalytically
40 active long-A pAgos have been implicated in host defense against invading nucleic acids such as plasmids and viruses
41 [14,15,24,25]. Besides, long-A pAgos function beyond host defense by stimulating homologous recombination [26,27] and
42 aiding in DNA replication [28]. No catalytically inactive long-A pAgos have been characterized to date. Much less is known
43 about long-B pAgos. All long-B pAgos lack the catalytic DEDX tetrad, and often the PAZ domain is partially truncated
44 (PAZ*) [5] (Box 1). The only canonical long-B pAgo that has been characterized to date is that of *Rhodobacter sphaeroides*
45 (RsAgo), which uses RNA guides to bind DNA targets [29]. Despite its lack of nuclease activity, RsAgo lowers expression
46 of plasmid-encoded genes and stimulates plasmid degradation in *E. coli* [29]. While the underlying mechanism is unclear,
47 it was hypothesized that binding of RsAgo to target plasmids may cause their transcriptional silencing, and/or recruitment
48 of nucleases that degrade the plasmids [29]. Another (non-canonical) long-B pAgo from *Archaeoglobus fulgidus* (AfAgo)
49 has been used as structural model for Ago and Ago-nucleic acid interactions [30,31]. However, AfAgo is truncated: it is
50 comprised of the MID and PIWI domains only (Figure 2I). As it can be considered to be a short pAgo, it will be discussed
51 in more details below.

52 While pAgo research has predominantly focused on the eAgo-like long-A pAgos, the majority (59%) of pAgos are 'short
53 pAgos' (Figure 1A) [5]. Like long-B pAgos, all short pAgos lack the DEDX tetrad required for target cleavage. Instead, they
54 genetically associate in operons with putative enzymes previously predicted to be nucleases (Figures 1 and 2D-G) [5–7].
55 As the MID-PIWI domains of eAgos were shown to be sufficient for guide-mediated target binding [32,33], it has been
56 hypothesized that short pAgo function in a modular host defense system, in which short pAgos act as guide-mediated
57 target binders, while relying on the associated enzymatic domains for target degradation [6]. In this review we will discuss
58 recent studies that uncovered that the functional mechanisms of short pAgos and their associated effector enzymes are
59 fundamentally distinct from long pAgos and eAgos [34–37].
60

61 Phylogeny of short pAgos

62 The majority of short pAgos form a distinct phylogenetic clade and strictly associate with proteins containing an "analog of
63 PAZ" (APAZ) domain [5,6,36,38] (Figure 1A and Box 1). However, we also find truncated pAgos scattered over different
64 branches of the long-A and long-B clades (Figure 1A) [5]. This implies that loss of the N- and PAZ domains occurred
65 multiple times in the evolution of pAgos [5]. Consequentially, not all short pAgos are phylogenetically related: The short
66 pAgo from *Sulfolobus islandicus* (SiAgo) and homologs thereof form a clade of pAgos that does not cluster with either long
67 or short pAgos (the SiAgo-like clade; Figure 1A), and short pAgo from *Archaeoglobus fulgidus* (AfAgo) clusters with long-
68 B clade pAgos (Figure 1A). SiAgo and AfAgo are not associated with APAZ domains, and rely on distinct functional
69 mechanisms (described below). Therefore, from here onward we refer to the phylogenetically clustered short pAgos
70 associated with APAZ domains as "short pAgos", and to other truncated pAgos as "pseudo-short pAgos".
71

72 94% of short pAgos are encoded by bacteria (proteobacteria (pseudomonadota): 54%, Bacteroidetes: 22%,
73 Actinobacteria: 8%, other bacterial phyla combined: 10%) and only 6% by archaea (Euryarchaeota: 6%, TACK group
74 archaea: 1%) (Figure 1B). Short pAgos can be divided in four phylogenetic clades: S1A, S1B, S2A, and S2B [36], and
75 based on their phylogeny, clade S2B short pAgos are further subdivided in nine subclades (S2B-1 to S2B-9; Figure 1).
76 The different (sub)clades of short pAgos are typically found in only a couple of prokaryotic phyla only (Figure 1B).
77

78 In all clades, short pAgos are encoded in operons that also encode an APAZ domain (Box 1). Initially, APAZ was predicted
79 to functionally replace the PAZ domain in long pAgos [7], but later studies suggested that it is homologous to the N-domain
80 of long Agos [39,40]. AlphaFold2-generated models [41] of short pAgo systems corroborate that the N domain and APAZ
81 are homologous and assume the same position respective to the MID-PIWI lobe (Figure 2, see also [35]). The N-terminus

82 of APAZ is generally fused to a (putative) catalytic domain [5] (Figure 2D-G). In clade S1A and S1B APAZ is fused to a
83 'Silent Information Regulator 2' (SIR2, also known as Sirtuin) domain (Figure 2D-E). In clade S2A APAZ is fused to a Toll-
84 interleukin-Receptor (TIR) domain (Figure 2F). In the different S2B subclades APAZ is fused to one of various domains
85 (e.g. Mrr-like, DUF4365 or DHS-like) (Figure 1B and Figure 2G) [5,36,42]. In clade S1A, the APAZ domain-containing
86 protein is fused to the N-terminus of short pAgo (Figure 2D). In other clades the APAZ-domain containing proteins are
87 encoded by a separate gene upstream of short pAgo (Figure 2E-G), which suggests functional interdependence. We refer
88 to short pAgo and its associated APAZ-domain containing protein as a 'short pAgo system'.
89

90 Like short pAgos, pseudo-short pAgos genetically co-localize with other proteins. For example, SiAgo is encoded in an
91 operon with a predicted transcriptional regulator, while two other proteins are encoded on the opposite DNA strand [34]
92 (Figure 2H). The presence of these three genes in close proximity of SiAgo is conserved for SiAgo homologs across
93 different strains [34]. AfAgo has so far only been characterized as a standalone protein [43], despite it being encoded in
94 an operon with two hypothetical proteins. Combined, this data suggests both short and pseudo-short pAgos function in
95 conjunction with proteins encoded in their genomic context.
96

97 Indeed, recent studies confirm that (pseudo-)short pAgos form complexes with their associated proteins to protect their
98 host against invading DNA such as plasmids and viruses [34–36]. Rather than triggering invader DNA degradation akin to
99 long pAgos, these (pseudo-)short pAgo systems function as abortive infection systems [44] that kill their host to prevent
100 replication and spread of the invader to others cells [34–37] (Figure 3). The diversified mechanisms on which these
101 (pseudo-)short pAgo systems rely are detailed below.

102 Functions and mechanisms of short pAgos

103 SPARSA systems

104 Short prokaryotic Argonaute/SIR2-APAZ (SPARSA, also known as Sir2/Ago) systems found in clades S1A (fused SIR2-
105 APAZ-pAgo) and S1B (co-encoded SIR2-APAZ and pAgo) are typified by the fusion of APAZ to a SIR2 domain (Figure 1
106 and Figure 2D-E) [5,36]. In eukaryotes, SIR2 proteins are involved in NAD⁺-dependent protein or histone deacetylation or
107 ADP-ribosylation, which can have implication for chromatin formation [45], DNA repair [46], and programmed cell death
108 [47]. In prokaryotes, SIR2 domains are NAD⁺-dependent deacetylases that play a role in stress resistance [48] and alter
109 the immune response of their hosts through histone deacetylation [49]. Besides, it was shown that several prokaryotic
110 abortive infection systems employ SIR2 to deplete NAD⁺ upon detection of invading DNA [37,50]. This causes cell death
111 of invaded cells, thereby preventing spread of the invader and providing population-based immunity (Figure 3).

112 Fused SPARSA systems from clade S1A (*Paraburkholderia graminis* (PgSPARSA) and *Joostella marina* (JomSPARSA)
113 as well as co-encoded clade S1B SPARSA systems (*Geobacter sulfurreducens* (GsSPARSA), *Caballeronia cordobensis*
114 (CcSPARSA) and *Xanthomonas vesicatoria* (XavSPARSA)) deplete NAD⁺ upon detection of invader DNA [35–37].
115 PgSPARSA, GsSPARSA and CcSPARSA provide protection against double stranded (ds)DNA phage lambda-vir, while
116 GsSPARSA and PgSPARSA also protect against dsDNA phage SECPhi27. GsSPARSA and CcSPARSA also provide
117 protection against transformation of plasmids containing a CloDF13 origin of replication (*ori*), but not against plasmids
118 containing other *oris* (ColA, p15A and RSF1030)[35]. For GsSPARSA, it was shown that invader interference critically
119 relies on both guide-binding by GsAgo and GsSIR2-APAZ NADase activity [35].

120 While GsSIR2-APAZ and GsAgo are encoded separately, the proteins form a heterodimeric complex [35]. When provided
121 with an RNA guide and complementary single stranded (ss)DNA target *in vitro*, the complex is activated and degrades
122 NAD⁺ (Figure 4). *In vivo*, GsSPARSA associates with small 20 nt long guide RNAs with a 5'-AU sequence. While most
123 guides are derived from genome-encoded genes, guides derived from plasmid-encoded transcripts are mostly obtained
124 from their *oris*, suggesting guide acquisition relies on RNA-dependent priming plasmid replication. Replication of the phage
125 lambda-vir relies on RNA-dependent priming as well [51], which might provide clues on how SPARSA obtains guides that

126 facilitate specific detection of plasmid- and viral invaders. Although other viruses and plasmids relying on the same
127 replication mechanism are not affected by SPARSA [35], it should be noted that many prokaryotic immune systems only
128 work against a subset of viruses and under specific conditions [50,52]. Combined, this shows that SPARSA provides
129 population-based immunity by triggering cell death through NAD⁺ depletion upon RNA-guided invader DNA detection
130 (Figure 4, Key Figure).

131 SPARTA systems

132 Short prokaryotic Argonaute/TIR-APAZ (SPARTA) systems make up clade S2A and are typified by the fusion of APAZ to
133 a TIR domain (Figure 1 and Figure 2F)[5,36]. TIR domains were originally identified as scaffolding proteins associated
134 with eukaryotic receptor proteins [53], but later they were found to possess NADase activity [54] which is important for
135 their immune function both in eukaryotes [55–60] and prokaryotes [50,61–63]. While some TIR domains deplete cellular
136 NAD⁺ and function as abortive infection systems (Figure 3), others generate signaling molecules (e.g. cyclic ADPR and v-
137 ADPR) to trigger downstream effects [50,54,55,64].

138 Akin to SPARSA, SPARTA systems from *Crenotalea thermophila* (CrtSPARTA) and *Maribacter polysiphoniae*
139 (MapSPARTA) degrade NAD⁺ (and NADP⁺) in the presence of plasmid DNA [36]. In contrast to SPARSA, however, no
140 direct interference with plasmid transformation was observed; instead, SPARTA lowers cell viability of plasmid-invaded
141 cells through NAD(P)⁺ depletion, removing invaded cells from bacterial cultures. Also, no SPARTA-mediated immunity
142 against bacteriophages was observed. While both SPARSA and SPARTA are short pAgo systems that degrade NAD⁺,
143 these differences suggest that SPARSA and SPARTA might rely on different mechanisms to detect invaders. However,
144 the different experimental conditions at which SPARSA and SPARTA have been functionality characterized could also
145 have played a role in the observed differences. Further research is required to establish differences and similarities
146 between SPARSA and SPARTA mechanisms.

147 As expected, the NAD(P)ase activity of SPARTA is attributed to the TIR domain of TIR-APAZ, which is catalytically active
148 in absence of the short pAgo partner [36]. In contrast to TIR domains that generate signaling molecules c-ADPR or v-
149 ADPR [50,54,55,64], SPARTA converts NAD(P)⁺ to non-cyclic ADPR(P) and NAM. In heterodimeric short pAgo/TIR-APAZ
150 complexes this activity is quenched, implying short pAgo controls the activity of TIR-APAZ. Through *in vitro* experiments
151 it was determined that guide RNA-mediated target ssDNA binding by SPARTA induces tetramerization of four guide/target-
152 bound SPARTA heterodimers, which reinstates the NAD(P)ase activity of the TIR domain (Figure 4). Oligomerization-
153 dependent activation of TIR domains is a general mechanism conserved from prokaryotic to eukaryotic immune systems
154 [61,62,65,66].

155 *In vivo*, SPARTA associates with 15-25 nt long guide RNAs with a 5'-A that are mostly derived from highly transcribed
156 genes encoded on multicopy plasmids [36]. In line with this observation, plasmids with a high copy number and/or encoding
157 highly transcribed genes activate SPARTA, whereas low copy plasmids lacking highly transcribed genes do not. Invading
158 DNA exploiting their host cell for propagation are often present in high copy numbers and highly transcribed. Combined,
159 this implies SPARTA senses invader activity through the high abundance of both their DNA and their RNA transcripts
160 which triggers its NAD(P)ase activity and consequentially cell death, thereby removing invaded cells from the bacterial
161 population (Figure 4).

162 S2B-clade short pAgo system from *Kordia jejudonensis*

163 S2B clade short pAgo systems are the most diverse in terms of distinct protein domains that are fused to APAZ, but they
164 are also the least explored: only the S2B system of *Kordia jejudonensis* has been studied *in vitro* [42] (Figure 1 and Figure
165 2G). The KjAgo-associated APAZ protein is fused to an Mrr-like domain [36] which is homologous to *E. coli* Mrr that acts
166 as a methylation-dependent DNA nuclease [67] (Figure 2). Akin to short pAgos from other clades [35,36], KjAgo forms a
167 heterodimeric complex with Mrr-APAZ [42]. *In vitro*, this complex catalyzes RNA/DNA guided cleavage of ssDNA targets,
168 but also non-specific cleavage of ssDNA and dsDNA [42]. No functional role of the KjAgo/Mrr-APAZ system was
169 determined, but it is conceivable that the KjAgo system mediates prokaryotic immunity akin to other short pAgo systems.

170 Yet, the results suggest that the KjAgo system relies on mechanisms that are clearly different from SPARSA and SPARTA:
171 upon its activation the KjAgo/Mrr-APAZ system might indiscriminately degrade nucleic acids to shut down the cell, an
172 abortive infection strategy that has been described for other prokaryotic immune systems (e.g. CBASS, CRISPR-Cas13,
173 type III CRISPR systems) [68–70]. Alternatively, the Mrr-like domain might compensate for loss of the catalytic activity of
174 the PIWI domain and specifically cleave guide-bound (invader) nucleic acids analogous to long-A pAgos and other
175 CRISPR-Cas systems [14,24,71–73].

176 Taken together, these studies show that short pAgos and their associated APAZ-domain containing proteins are fused or
177 form heterodimeric complexes (Figure 2D-G, Figure 4). The fact that fusion of short pAgos with their associated APAZ-
178 effectors occurred multiple times in evolution underscores the importance of their complexation. In short pAgo systems,
179 the short pAgo acts as a ‘sensor’ that facilitates guide-mediated recognition and binding of nucleic acid invaders. Upon
180 target binding, the APAZ-fused domain is catalytically activated and acts as an ‘effector’. In SPARSA and SPARTA
181 systems, target detection results in unleashed SIR2- or TIR-mediated NAD(P)ase activity that consequentially kills the
182 host of the invaded cells (Figure 3, Figure 4). For clade S2B short pAgos the exact catalytic mechanism activated and the
183 consequences thereof remain to be determined.

184 Functions and mechanisms of pseudo-short pAgos

185 *Sulfolobus islandicus* pAgo

186 The archaeal SiAgo and homologs thereof do not cluster with either long or short pAgos, but form a separate branch in
187 the phylogenetic pAgo tree (Figure 1). SiAgo functionality relies on two genetically associated proteins (Figure 1 and Figure
188 2H): Ago associated protein 1 (SiAga1) and Ago associated protein 2 (SiAga2) [34]. These three proteins together function
189 as a prokaryotic immune system that protect its host against infection of the dsDNA virus SMV1 [34]. Akin to short pAgos,
190 SiAgo and SiAga1 form heterodimeric complexes upon their co-expression [34]. However, SiAgo and SiAga1 alone do not
191 confer defense against bacteriophages: they additionally rely on the effector Aga2. Aga2 is a membrane protein that forms
192 large oligomeric complexes and binds phospholipids. While SiAgo-Aga1 complexes reside in the cytoplasm, Aga2 mostly
193 localizes in the membrane. Upon viral infection, the SiAgo-Aga1 complex is directed to the membrane, triggering activation
194 of Aga2. This results in loss of membrane polarity and consequentially triggers cell death in invaded cells [34].

195 While *in vitro* SiAgo appears to bind RNA guides, the SiAgo-SiAga1 complex associates with all guide/target type
196 (DNA/RNA) combinations, [34]. However, it is unknown what combination of guides/target type activates the system
197 [34]. Nevertheless, a model is proposed wherein the SiAgo-SiAga1 complex recognizes invading nucleic acids through
198 guide-target binding, consequentially activating Aga2 to initiate abortive infection [34]. Contrary to short pAgo systems,
199 the SiAgo system does not seem to target plasmids in the reported experimental setup: overexpression of genes from
200 plasmids does not cause substantial Aga2 activation. In conclusion, although it relies on different accessory proteins than
201 short pAgos, also the SiAgo system mediates population-based immunity by abortive infection upon detection of invading
202 DNA (Figure 4).

203 *Archaeoglobus fulgidus* pAgo

204 AfAgo is a truncated long-B pAgo that is comprised of the MID and PIWI domains only [74] (Figure 1, Figure 2I). AfAgo
205 was one of the first Ago proteins to be crystalized and served as a model to study Ago-nucleic acid interactions [75]. In
206 these structures AfAgo crystallizes as a homodimer, but the functional relevance of AfAgo dimerization remained unknown.
207 A recent study showed that AfAgo also forms dimers in solution, and that dimerization is stabilized upon binding of dsDNA
208 ends [43]. As each AfAgo component in the dimer can accommodate a separate dsDNA end, AfAgo dimers can stimulate
209 formation of DNA loops. This suggests that AfAgo might be involved in DNA repair or integration of mobile genetic
210 elements. Also long-A pAgos have been implicated in homologous recombination [26,27], but there are no indications that
211 the dimerization is required in this process. Although its natural preferences for DNA/RNA have not been studied, AfAgo
212 interacts with both RNA and DNA *in vitro* [75]. It is also unknown if AfAgo, like other pAgos, acts as host defense system.

213 Akin to other (pseudo-) short pAgos, AfAgo is encoded in an operon that also encodes hypothetical proteins. Further
214 experimentation is required to determine the biological function of AfAgo.

215 Concluding remarks

216 Short pAgos and pseudo-short pAgos are prokaryotic Argonaute proteins comprised of the MID and PIWI domains only,
217 lack catalytic activity, and can have different phylogenetic origins. As they retain their ability to use guides to bind
218 complementary targets, they serve as 'sensors' that detect invading DNA. All (pseudo-)short pAgos functionally
219 characterized thus far mediate abortive infection (Figure 3): They form a complex with 'effector' proteins that are activated
220 upon guide-mediated invader detection, thereby killing their host in order to protect neighbouring cells (Figure 4).

221 Despite the major advances in understanding of (pseudo-)short pAgo functionality, many aspects of their functionality
222 remain mysterious (see Outstanding questions). It is unknown how (pseudo-)short pAgos interact with their effector
223 partners. As the APAZ domain associated with short pAgos is homologous to the N domain found in long pAgos and
224 eAgos, it might facilitate interactions with short pAgo and/or play a role in guide loading and/or target release. However, it
225 is also conceivable that APAZ serves to activate the effector domain upon guide-mediated target binding by Ago,
226 presumably through a conformational change. Likewise, in the SiAgo system, SiAga1 may connect SiAgo to SiAga2 in
227 response to guide-mediated target binding, which induces membrane depolarization by Aga2. Besides, the SiAgo/SiAga1
228 complex showed increased affinity for nucleic acids compared to the SiAgo monomer, which suggests that SiAga1 either
229 aids in binding guide and/or target nucleic acids or induces a conformation of SiAgo to favor nucleic acid binding. Structure-
230 derived insights into protein-protein and protein-nucleic acid interactions are required to reveal the role of APAZ in short
231 pAgo systems and Aga1 in the SiAgo system, and could illuminate the mechanism by which (pseudo-)short pAgos control
232 the activity of their associated effectors.

233 Short pAgos characterized to date utilize small RNA guides to DNA, but it remains largely unknown how (pseudo-)short
234 pAgos distinguish self (genomic DNA) from non-self (invader DNA). Potentially, guide RNA biogenesis specifically yields
235 invader-targeting guide RNAs. In contrast with that hypothesis, both short and long-B pAgos acquire guide RNAs from the
236 entire transcriptome [29,35,36], which results in the loading of self-targeting guide RNAs. Yet, these observations were
237 made while overexpressing the pAgos in heterologous hosts, and it cannot be ruled out guide RNA biogenesis and loading
238 is more specific in the natural host under native expression conditions. Eukaryotes have dedicated pathways for guide
239 RNA biogenesis: In general eAgoOs are loaded with microRNA (miRNA) or small interfering RNA (siRNA) guides that are
240 generated from dsRNA substrates such as RNA hairpins or bidirectional transcripts by the RNase III family proteins Dicer
241 and/or Drosha [76–78]. PIWIs bind PIWI-interacting RNAs (piRNA) guides that are derived from transcripts of piRNA
242 clusters to target transposon transcripts, or secondary piRNAs that are generated from targeted transposon transcripts in
243 an ePIWI-dependent manner [79]. While prokaryotes lack Dicer and Drosha homologs, bacteria encode simpler RNase III
244 family proteins [13] as well as an array of other housekeeping RNases that could play a role in guide RNA biogenesis.
245 Analogous to the ePIWI pathway, CRISPR-Cas systems rely CRISPR RNA guides (crRNAs) derived from transcripts of
246 CRISPR loci to target nucleic acid invaders [80]. Although some pAgos are encoded in the context of Cas genes [5,6,38],
247 so far, no association has been found between crRNA guides and pAgos. While (pseudo-)short pAgos do not strictly rely
248 on genome-encoded small RNAs [35,36], it can also not be ruled out that certain pAgo hosts encode precursors of invader-
249 targeting guide RNAs on the genome.

250 Besides preferential guide generation, the availability of target DNA might play a role in differentiating self and non-self
251 DNA. All (pseudo-)short pAgos reported to date target ssDNA *in vitro*, but act on dsDNA invaders *in vivo* [34–36]. Being
252 unable to unwind dsDNA targets, pAgos might rely on other enzymes or processes (e.g. replication or transcription) to
253 make DNA susceptible for detection. If such process or enzymes are different for genomic and invading DNA, they could
254 contribute to invader-specific targeting by pAgos. Resolving the mechanisms facilitating pAgo-mediated dsDNA
255 recognition can therefore contribute to understanding how pAgos distinguish self from non-self.

256 The majority of the vast (pseudo-)short pAgo-diversity await exploration. For example, certain S2A clade TIR-APAZ
257 domains are additionally fused to an Mrr domain (Figure 2), and many S2B-clade short pAgos associate with domains of
258 which the functions are not clear. For most pseudo-short pAgos the genetic context is yet to be investigated. Besides,
259 more distant pAgos homologs have been identified (e.g. PIWI-RE [6,81] and DdmE [82]). With the rapidly expanding
260 metagenomics data available it is not unlikely that additional clades containing distinct (pseudo-)short or long pAgos or
261 more distantly related homologs thereof will be discovered in the near future. Characterization of pAgo variants will
262 determine what functional roles they can fulfil, which mechanism they convey, and what evolutionary turns pAgos have
263 taken.

264 Finally, short pAgo systems can be isolated and programmed with short (synthetic) RNA guides with sequences of choice,
265 akin to CRISPR-Cas systems [83–86] and long pAgos [87]. As target binding triggers a specific catalytic activity, they
266 could be repurposed for a range of sequence-specific applications. For example, SPARTA has been repurposed for the
267 detection of ssDNA and dsDNA sequences [36]. Possibly, other pAgo systems with a distinct catalytic activity could be
268 repurposed for targeted nucleic acid modification or genome editing. As such, the characterization (pseudo-)short pAgos
269 not only uncovered a novel, highly diverse class of immune systems, but it could also inspire a new generation of
270 programmable molecular tools.

271

272

273

274

275

276

277

278

279

280

281

282

283

284

285

286

287 **BOX 1**

288 The characteristics of pAgo domains and other structural features of Agos are described in this box.

289 **MID**

290 The MID (Middle) domain forms a pocket that in most pAgos contains four conserved residues (Y/R, K, Q
291 and K [5]) and coordinates a divalent cation [75] which together anchor the 5'-phosphate (5'-P) group of
292 the guide. Certain pAgos preferentially bind 5'-hydroxylated (5'-OH) guides instead, which is attributed to
293 a more hydrophobic binding pocket and absence of the divalent cation [5,11], while other pAgos show no
294 clear preference for 5'-P or 5'-OH guides [21,22]. The 5'-nucleotide of the guide is also bound in the MID
295 domain pocket (sometimes in a sequence-specific manner [88]), and therefore it is unavailable for base-
296 pairing with the target.

297 **PIWI(*)**

298 The PIWI (P-element-Induced Wimpy Testis) domain is homologous to RNase H, which cleaves the RNA
299 strand of RNA/DNA substrates [89]. In Agos, the PIWI domain coordinates and pre-orders the 'seed'
300 nucleotides of the guide (nucleotide 2-7 or 2-8) in a helical conformation with bases exposed to the solvent
301 [90]. This promotes guide/target base pairing by lowering the entropic costs of duplex formation. PIWI is
302 also the domain responsible for target cleavage (slicing): Slicing Agos contain a DEDX motif (see DEDX) in
303 the PIWI domain, while this motif is mutated in Agos that rely on target binding for their function. PIWI
304 domains lacking the DEDX tetrad are referred to as PIWI*.

305 **DEDX catalytic tetrad**

306 The DEDX motif (where X denotes D, H or, K) found in the PIWI domain of slicing Agos facilitates target
307 strand cleavage. The glutamic acid residue is located on a structural feature termed the glutamate finger
308 [91] that completes the catalytic tetrad upon target binding. The DEDX tetrad coordinates two divalent
309 cations that catalyse hydrolysis of the target strand phosphate backbone between nucleotides 10 and 11
310 [92]. Most eAgos from the AGO clade, some long-A pAgos, and long-B and (pseudo-)short pAgos have
311 mutations in the DEDX motif that abolish cleaving activity [5]. However, even in slicing Agos target
312 cleavage can be affected by mismatches between the guide and the target [93,94].

313 **MID-PIWI (PIWI lobe)**

314 The MID and PIWI domains together form the PIWI lobe, which is sufficient for guide-mediated target
315 binding and cleavage [32,33]. In line with their functional importance, these domains show the highest
316 conservation over Agos from all domains of life, and it are the only domains found in all Argonaute family
317 proteins [6,95]. Short pAgos are generally comprised of the MID-PIWI domains only.

318 **N domain**

319 The N domain is the least conserved domain in Agos and functions in guide loading and target cleavage:
320 It acts as a wedge to facilitate removal of the passenger strand during guide loading and removal of cleaved
321 target strands in slicing Agos [96,97].

322 **PAZ(*)**

323 The PAZ (PIWI-Argonaute-Zwille) domain interacts with the 3' end of the guide protecting it from
324 degradation [33]. The PAZ domain usually displays no sequence preference, although PAZ domains of
325 ePIWIs specifically recognize methylated 3' ends [98]. Upon guide-mediated target binding, the 3'-end of
326 the guide is released from the PAZ domain [99,100]. The associated conformational changes result in
327 target cleavage. All long-B pAgos and some long-A pAgos have a truncated PAZ domain which is referred
328 to as PAZ* [5]. In PAZ* the guide 3' end binding pocket is at least partially lost [101,102]. Possibly, this
329 allows for more extensive duplex formation between the guide and the target [101,102].

330

331 **N-PAZ (N lobe)**

332 The N and PAZ domains together form the N lobe, which is not required for guide-mediated target binding
333 but enhances on-target cleavage specificity [32,33]. All (pseudo-)short pAgos lack the N lobe [5].

334 **APAZ**

335 Short pAgos lack both the N and PAZ domains, but are generally co-encoded in an operon or fused to an
336 Analogue of PAZ (APAZ) domain-containing protein. The APAZ domain is usually fused to a variable
337 catalytic domain (Figure 2) [5–7]. The APAZ domain was originally thought to be a functional analogue of
338 the PAZ domain [7]. However, other predictions [39,40] as well as Alphafold2 modeling (Figure 2) show that
339 at least part of the APAZ domain is homologous to the N domain instead. Furthermore, the Alphafold2
340 models suggest that APAZ assumes the same position respective to the MID-PIWI domains as the N-PAZ
341 domains in long pAgos. The function of APAZ is currently unknown: it could have a ‘wedging’ function like
342 the N domain, control short pAgo-mediated activation of the effector domain, or it could have another
343 unknown function.

344

345

346

347

348

349

350

351

352

353

354

355

356

357

358

359

360

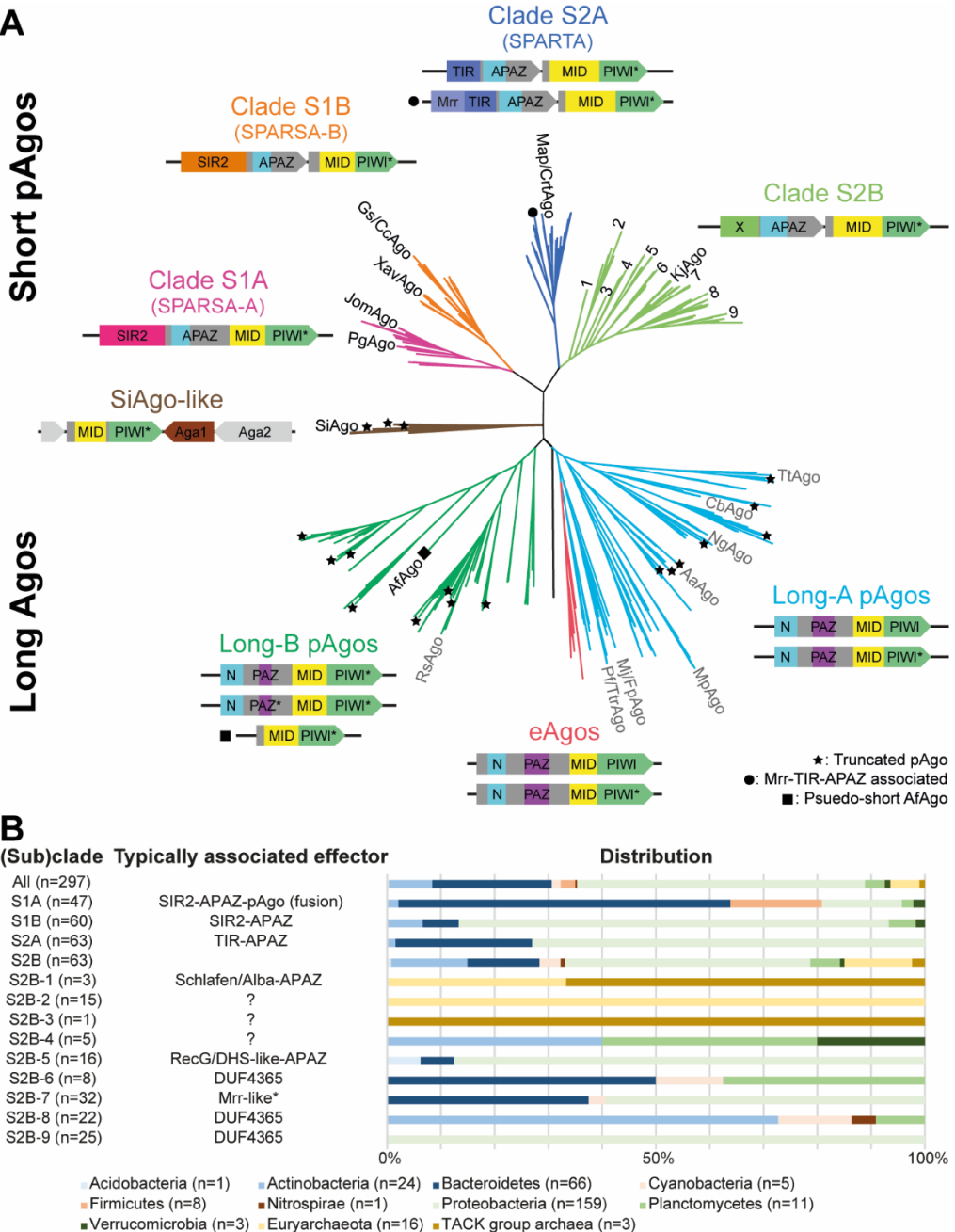
361

362

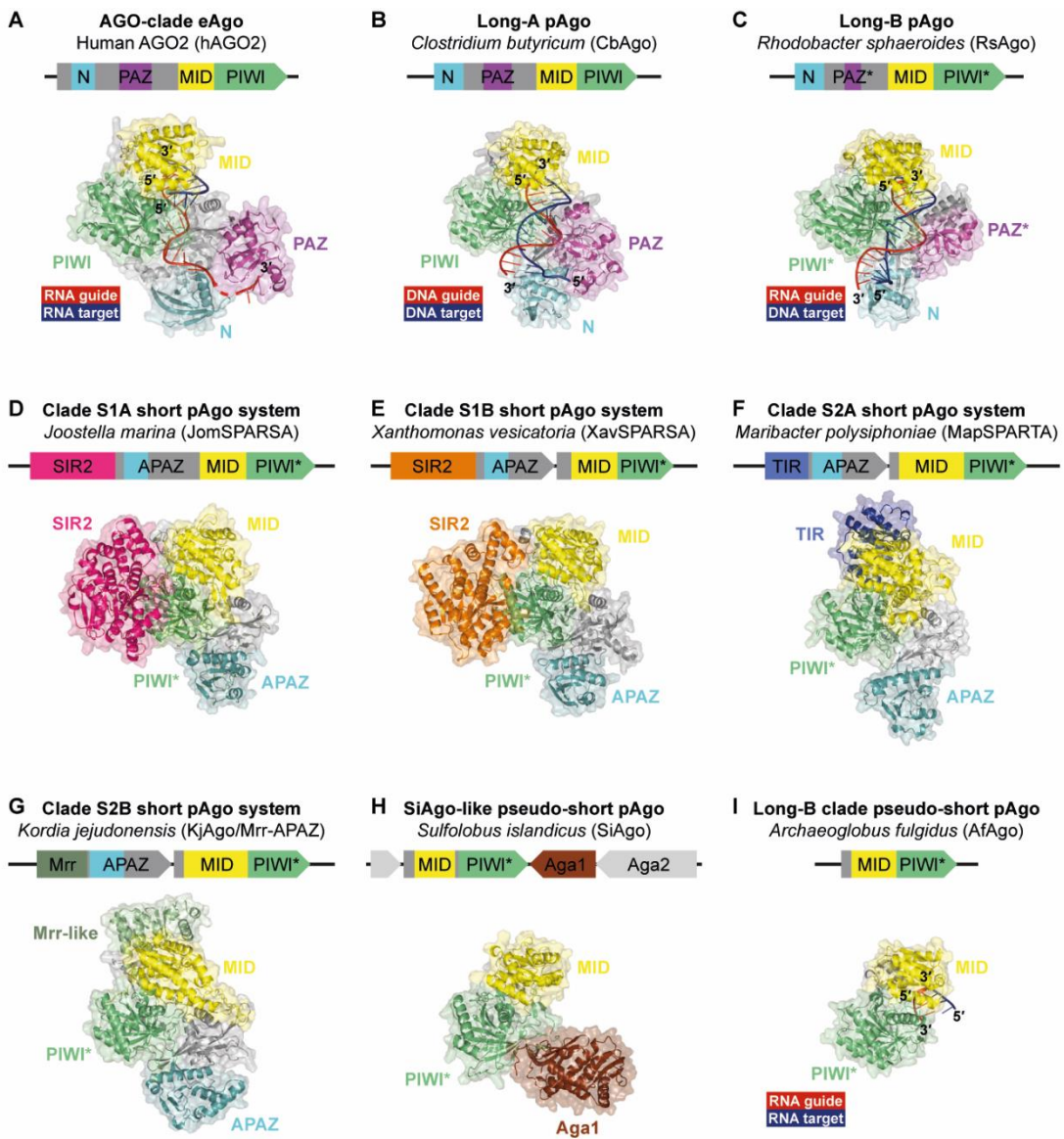
363

364

365

368 **Figure 1 Phylogeny of prokaryotic Argonaute proteins.**

369 (A) Maximum-likelihood-based unrooted phylogenetic tree containing all bacterial and archaeal pAgo homologs identified in the
 370 RefSeq database containing at least scaffold-level assemblies, as well as selected experimentally characterized pAgos, eAgos,
 371 and SiAgo homologs. Analysis performed as previously [36]. Clade S1A: SIR2-APA2-pAgo fusion (SPARSA-A). Clade S1B:
 372 operon with pAgo and SIR2-APA2 (SPARSA-B). Clade S2A: operon with pAgo and TIR-APA2 (SPARTA). Clade S2B: operon
 373 with pAgo and APA2 fused to one of various domains (denoted 'X'), including Mrr, DUF4365, and DHS-like domains (see also
 374 panel B). ★: truncated pAgos in Long-A, Long-B, and SiAgo-like clades. ●: Short pAgos associated with Mrr-TIR-APA2. ■: Psuedo-
 375 short AfAgo. The fully annotated tree can be downloaded from Mendeley Data (<https://dx.doi.org/10.17632/mpgn9by7z2.1>).
 376 (B) Typically associated effector domains and distribution of 297 short pAgo systems from panel A. Typically putative associated
 377 effectors domains as identified by InterPro (identified in >50% of short pAgo systems in this specific clade). Schlafen/Alba:
 378 IPR038461. RecG: IPR038475. DHS-like: IPR029035. DUF4365: IPR025375. ?: Effector domain not identified by InterPro. *:
 379 The Mrr-like domain in clade S2B-7 effector proteins is not identified by InterPro but is based on earlier studies [42] and
 380 AlphaFold2 predictions (Figure 2) [41,103].



381

382 **Figure 2** Operon structure, domain composition, and (predicted) structural architecture of prokaryotic Argonaute
383 proteins.

384 Crystal structures of (A) human AGO2 (PDB: 4W5O), (B) *Clostridium butyricum* long-A pAgo (CbAgo; PDB: 6QZK), (C)
385 *Rhodobacter sphaeroides* long-B pAgo (PDB: 5AWH), and (I) *Archaeoglobus fulgidus* truncated long-B pAgo (PDB: 1YTU) in
386 complex with guide and target strands, and Alphafold2-predicted models [41] for (pseudo-)short pAgo systems from distinct
387 phylogenetic clades including (D) clade S1A *Joostella marina* SPARSA (JomSPARSA), (E) clade S2B *Xanthomonas vesicatoria*
388 SPARSA (XavSPARSA), (F) clade S2A *Maribacter polysiphoniae* SPARTA (MapSPARTA), (G) the clade S2B *Kordia jejudonensis*
389 (KjAgo/Mrr-APAZ) system, and (H) the pseudo-short *Sulfolobus islandicus* (SiAgo-SiAga1-SiAga2) system. The related
390 (predicted) domain composition (with corresponding colors) and operon structure are given above each structural model.
391 Explanation of domain functions are given in Box 1. Alphafold2 predictions can be downloaded from Mendeley Data
392 (<https://dx.doi.org/10.17632/mpgn9by7z2.1>).

393

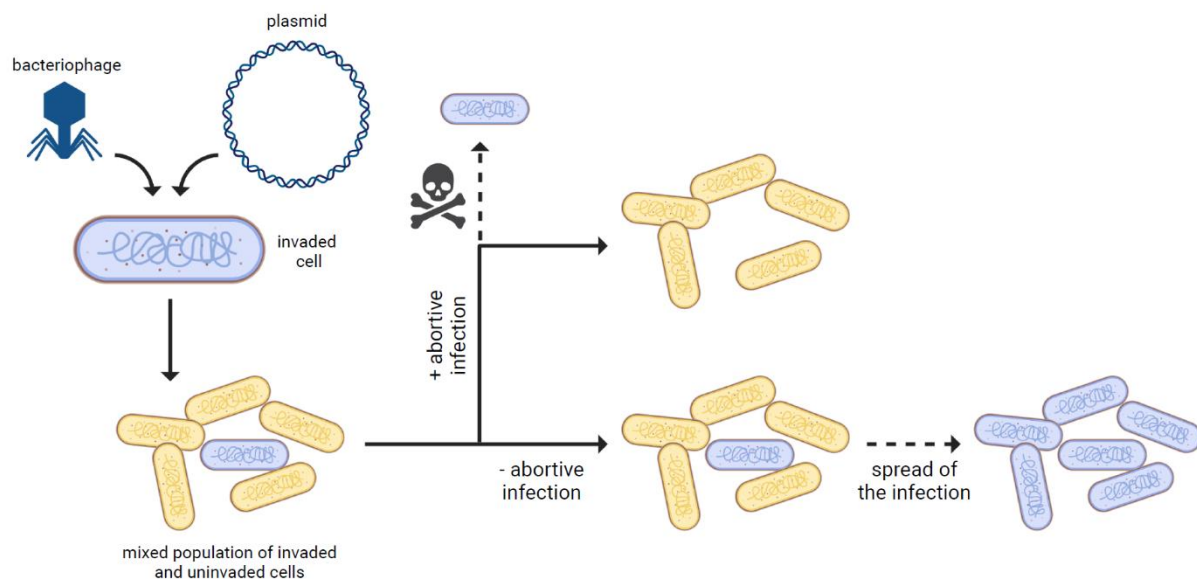
394

395

396

397

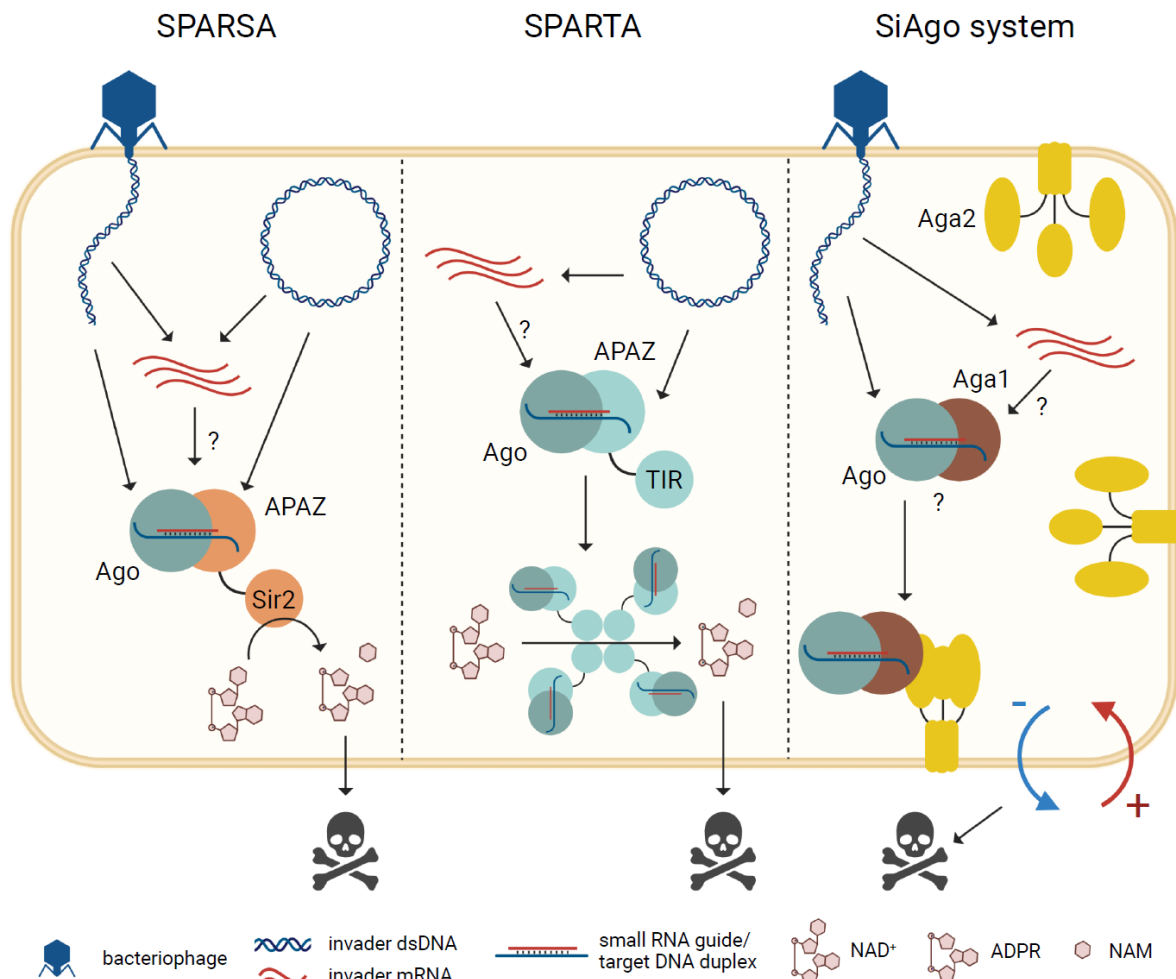
398



399

400 **Figure 3 General mechanism of Abortive infection systems**

401 Invading nucleic acid such as phages or plasmids can enter prokaryotic cells and, in absence of abortive infection systems, may
 402 persist in the population, providing a metabolic burden, or they can spread to neighboring cells through lysis and infection of
 403 neighboring cells (phages), or through conjugation (conjugative plasmids). Abortive infection systems prevent spread of invading
 404 nucleic acids by sensing the invader and subsequently killing their host cell. This will remove invaded cells from the population.
 405 This figure was created using BioRender (<https://biorender.com/>).
 406



407
408
409
410
411
412
413
414
415
416
417
418
419

Figure 4 Schematic representation of host defense against invading DNA by (pseudo-) short pAgo systems.

Short pAgos from SPARSA (left), SPARTA (middle), and pseudo-short SiAgo (right) systems form heterodimeric complexes with their accessory effector proteins. Invading viral and plasmid dsDNA (blue) enter the cell, after which the (pseudo-)short pAgo system acquires small guide RNAs from invader RNA transcripts (red) by an unknown mechanism. The guide RNA facilitates sequence-specific recognition of invading DNA strands (blue) which results in catalytic activation of the effector domains: SIR2 (SPARSA), TIR (SPARTA), or Aga2 (SiAgo system). In SPARSA and SPARTA, SIR2/TIR activation leads to the conversion of NAD(P)⁺ to NAM and ADPR(P). In SPARTA, catalytic activation requires tetramerization of four guide/target-bound heterodimeric SPARTA complexes. Upon invader detection, the SiAgo-SiAgo1 complex is recruited to the membrane protein SiAgo2 which induces membrane depolarization. Both NAD(P)⁺ depletion and membrane depolarization induce cell death, which protects neighboring cells and cures metabolically costly plasmids from the population (see also Figure 3). This figure was created using BioRender (<https://biorender.com/>).

Acknowledgements

This work was supported by a Netherlands Organization for Scientific Research (NWO) VENI grant (016.Veni.192.072) and a European Research Council (ERC) starting grant (ERC-2020-STG 948783) to D.C.S.

Declaration of interests

D.C.S. and B.K. (together with Ana Potocnik) submitted a patent application regarding the utilization of short pAgo systems for nucleic acid detection.

426 **References**

427 [1] G. Meister, Argonaute proteins: functional insights and emerging roles, *Nat. Publ. Gr.* 14 (2013) 447.
428 <https://doi.org/10.1038/nrg3462>.

429 [2] D.M. Ozata, I. Gainetdinov, A. Zoch, D. O'Carroll, P.D. Zamore, PIWI-interacting RNAs: small RNAs with big functions,
430 *Nat. Rev. Genet.* 20 (2019) 89–108. <https://doi.org/10.1038/s41576-018-0073-3>.

431 [3] H. Vaucheret, Plant ARGONAUTES, *Trends Plant Sci.* 13 (2008) 350–358.
432 <https://doi.org/10.1016/j.tplants.2008.04.007>.

433 [4] J. Sheu-Gruttaduria, I.J. MacRae, Structural Foundations of RNA Silencing by Argonaute, *J. Mol. Biol.* 429 (2017)
434 2619–2639. <https://doi.org/10.1016/j.jmb.2017.07.018>.

435 [5] S. Ryazansky, A. Kulbachinskiy, A.A. Aravin, The Expanded Universe of Prokaryotic Argonaute Proteins, *MBio.* 9
436 (2018) e01935-18. <https://doi.org/10.1128/mBio.01935-18>.

437 [6] D.C. Swarts, K. Makarova, Y. Wang, K. Nakanishi, R.F. Ketting, E. V. Koonin, D.J. Patel, J. Van Der Oost, The
438 evolutionary journey of Argonaute proteins, *Nat. Struct. Mol. Biol.* 21 (2014) 743–753.
439 <https://doi.org/10.1038/nsmb.2879>.

440 [7] K.S. Makarova, Y.I. Wolf, J. van der Oost, E. V. Koonin, Prokaryotic homologs of Argonaute proteins are predicted to
441 function as key components of a novel system of defense against mobile genetic elements, *Biol. Direct.* 4 (2009).
442 <https://doi.org/10.1186/1745-6150-4-29>.

443 [8] K.S. Makarova, Y.I. Wolf, S. Snir, E. V. Koonin, Defense Islands in Bacterial and Archaeal Genomes and Prediction of
444 Novel Defense Systems, *J. Bacteriol.* 193 (2011) 6039. <https://doi.org/10.1128/JB.05535-11>.

445 [9] G. Sheng, H. Zhao, J. Wang, Y. Rao, W. Tian, D.C. Swarts, J. Van Der Oost, D.J. Patel, Y. Wang, Structure-based
446 cleavage mechanism of *Thermus thermophilus* argonaute DNA guide strand-mediated DNA target cleavage, *Proc. Natl.*
447 *Acad. Sci. U. S. A.* 111 (2014) 652–657. <https://doi.org/10.1073/pnas.1321032111>.

448 [10] U.J. Rashid, D. Paterok, A. Koglin, H. Gohlke, J. Piehler, J.C.H. Chen, Structure of *Aquifex aeolicus* argonaute
449 highlights conformational flexibility of the PAZ domain as a potential regulator of RNA-induced silencing complex
450 function, *J. Biol. Chem.* 282 (2007) 13824–13832. <https://doi.org/10.1074/jbc.M608619200>.

451 [11] E. Kaya, P.J. Kranzusch, R.C. Wilson, S.C. Strutt, K.R. Knoll, K.W. Doxzen, J.A. Doudna, A bacterial Argonaute with
452 noncanonical guide RNA specificity, *Proc. Natl. Acad. Sci.* 113 (2016) 4057–4062.
453 <https://doi.org/10.1073/pnas.1524385113>.

454 [12] J.W. Hegge, D.C. Swarts, S.D. Chandradoss, T.J. Cui, J. Kneppers, M. Jinek, C. Joo, J. Van Der Oost, DNA-guided
455 DNA cleavage at moderate temperatures by *Clostridium butyricum* Argonaute, *Nucleic Acids Res.* 47 (2019) 5809–
456 5821. <https://doi.org/10.1093/nar/gkz306>.

457 [13] S.A. Shabalina, E. V. Koonin, Origins and evolution of eukaryotic RNA interference, *Trends Ecol. Evol.* 23 (2008) 578–
458 587. <https://doi.org/10.1016/j.tree.2008.06.005>.

459 [14] D.C. Swarts, M.M. Jore, E.R. Westra, Y. Zhu, J.H. Janssen, A.P. Snijders, Y. Wang, D.J. Patel, J. Berenguer, S.J.J.
460 Brouns, J. Van Der Oost, DNA-guided DNA interference by a prokaryotic Argonaute, *Nature.* 507 (2014) 258–261.
461 <https://doi.org/10.1038/nature12971>.

462 [15] D.C. Swarts, J.W. Hegge, I. Hinojo, M. Shiiomori, M.A. Ellis, J. Dumrongkulraksa, R.M. Terns, M.P. Terns, J. Van Der

463 Oost, Argonaute of the archaeon *Pyrococcus furiosus* is a DNA-guided nuclease that targets cognate DNA, *Nucleic*
464 *Acids Res.* 43 (2015) 5120–5129. <https://doi.org/10.1093/nar/gkv415>.

465 [16] A. Zander, S. Willkomm, S. Ofer, M. Van Wolferen, L. Egert, S. Buchmeier, S. Stöckl, P. Tinnefeld, S. Schneider, A.
466 Klingl, S.V. Albers, F. Werner, D. Grohmann, Guide-independent DNA cleavage by archaeal Argonaute from
467 *Methanocaldococcus jannaschii*, *Nat. Microbiol.* 2 (2017). <https://doi.org/10.1038/nmicrobiol.2017.34>.

468 [17] K.Z. Lee, M.A. Mechikoff, A. Kikla, A. Liu, P. Pandolfi, K. Fitzgerald, F.S. Gimble, K. V Solomon, NgAgo possesses
469 guided DNA nicking activity, *Nucleic Acids Res.* 49 (2021) 9926–9937. <https://doi.org/10.1093/nar/gkab757>.

470 [18] Y. Ishino, L. Zhang, Q. Liu, Y. Feng, X. Guo, Y. Sun, L. Chen, F. Huang, Hyperthermophilic Argonaute From
471 *Ferroglobus placidus* With Specificity on Guide Binding Pattern, *Microbiol.* 12 (2021) 654345.
472 <https://doi.org/10.3389/fmicb.2021.654345>.

473 [19] K.W. Doxzen, J.A. Doudna, DNA recognition by an RNA-guided bacterial Argonaute, *PLoS One.* 12 (2017) 1–14.
474 <https://doi.org/10.1371/journal.pone.0177097>.

475 [20] L. Lisitskaya, Y. Shin, A. Agapov, A. Olina, E. Kropocheva, S. Ryazansky, A.A. Aravin, D. Esyunina, K.S. Murakami, A.
476 Kulbachinskiy, Programmable RNA targeting by bacterial Argonaute nucleases with unconventional guide binding and
477 cleavage specificity, *Nat. Commun.* 2 (2022) 1–15. <https://doi.org/10.1038/s41467-022-32079-5>.

478 [21] W. Li, Y. Liu, R. He, L. Wang, Y. Wang, W. Zeng, Z. Zhang, F. Wang, L. Ma, A programmable pAgo nuclease with
479 RNA target preference from the psychrotolerant bacterium *Mucilaginibacter paludis*, *Nucleic Acids Res.* 50 (2022)
480 5226–5238. <https://doi.org/10.1093/nar/gkac315>.

481 [22] L. Wang, X. Xie, Y. Liu, W. Li, B. Lv, Z. Zhang, J. Yang, G. Yan, W. Chen, C. Zhang, F. Wang, L. Ma, A bacterial
482 Argonaute with efficient DNA and RNA cleavage activity guided by small DNA and RNA, *BioRxiv*. (2021).

483 [23] E. Kropocheva, A. Kuzmenko, A.A. Aravin, D. Esyunina, A. Kulbachinskiy, A programmable pAgo nuclease with
484 universal guide and target specificity from the mesophilic bacterium *Kurthia massiliensis*, *Nucleic Acids Res.* 49 (2021)
485 4054–4065. <https://doi.org/10.1093/nar/gkab182>.

486 [24] A. Kuzmenko, A. Ogienko, D. Esyunina, D. Yudin, M. Petrova, A. Kudinova, O. Maslova, M. Ninova, S. Ryazansky, D.
487 Leach, A.A. Aravin, A. Kulbachinskiy, DNA targeting and interference by a bacterial Argonaute nuclease, *Nature.* 587
488 (2020) 632–637. <https://doi.org/10.1038/s41586-020-2605-1>.

489 [25] D.C. Swarts, M. Szczepaniak, G. Sheng, S.D. Chandradoss, Y. Zhu, E.M. Timmers, Y. Zhang, H. Zhao, J. Lou, Y.
490 Wang, C. Joo, J. van der Oost, Autonomous Generation and Loading of DNA Guides by Bacterial Argonaute, *Mol. Cell.*
491 65 (2017) 985–998.e6. <https://doi.org/10.1016/j.molcel.2017.01.033>.

492 [26] L. Fu, L. Han, Y. Xiang, C. Xie, M. Jin, The prokaryotic Argonaute proteins enhance homology sequence-directed
493 recombination in bacteria, *Nucleic Acids Res.* 47 (2019) 3568–3579. <https://doi.org/10.1093/nar/gkz040>.

494 [27] D. Esyunina, A. Okhtienko, A. Olina, M. Prostova, A.A. Aravin, A. Kulbachinskiy, Specific targeting of plasmids with
495 Argonaute enables genome editing, (2022) 1–24.

496 [28] S.M. Jolly, I. Gainetdinov, K. Jouravleva, H. Zhang, L. Strittmatter, S.M. Bailey, G.M. Hendricks, A. Dhabaria, B.
497 Ueberheide, P.D. Zamore, *Thermus thermophilus* Argonaute Functions in the Completion of DNA Replication, *Cell.* 182
498 (2020) 1545–1559.e18. <https://doi.org/10.1016/j.cell.2020.07.036>.

499 [29] I. Olovnikov, K. Chan, R. Sachidanandam, D.K. Newman, A.A. Aravin, Bacterial Argonaute Samples the Transcriptome
500 to Identify Foreign DNA, *Mol. Cell.* 51 (2013) 594–605. <https://doi.org/10.1016/j.molcel.2013.08.014>.

501 [30] J.S. Parker, E.A. Parizotto, M. Wang, S.M. Roe, D. Barford, Enhancement of the Seed-Target Recognition Step in RNA
502 Silencing by a PIWI/MID Domain Protein, *Mol. Cell.* 33 (2009) 204–214. <https://doi.org/10.1016/j.molcel.2008.12.012>.

503 [31] J.B. Ma, K. Ye, D.J. Patel, Structural basis for overhang-specific small interfering RNA recognition by the PAZ domain,
504 *Nature*. 429 (2004) 318–322. <https://doi.org/10.1038/nature02519>.

505 [32] D.M. Dayeh, B.C. Kruithoff, K. Nakanishi, Structural and functional analyses reveal the contributions of the C- and N-
506 lobes of Argonaute protein to selectivity of RNA target cleavage, *J. Biol. Chem.* 293 (2018) 6308–6325.
507 <https://doi.org/10.1074/jbc.RA117.001051>.

508 [33] J.K. Hur, M.K. Zinchenko, S. Djuranovic, R. Green, Regulation of Argonaute slicer activity by guide RNA 3' end
509 interactions with the N-terminal lobe, *J. Biol. Chem.* 288 (2013) 7829–7840. <https://doi.org/10.1074/jbc.M112.441030>.

510 [34] Z. Zeng, Y. Chen, R. Pinilla-Redondo, S. A Shah, F. Zhao, C. Wang, Z. Hu, C. Zhang, R.J. Whitaker, Q. She, W. Han,
511 A Short Prokaryotic Argonaute Activates Membrane Effector to Confer Antiviral Defense, *Cell Host Microbe Microbe*.
512 (2022) 1–14. <https://doi.org/10.2139/ssrn.3988392>.

513 [35] M. Zaremba, D. Dakineviciene, E. Golovinas, E. Zagorskaité, E. Stankunas, A. Lopatina, R. Sorek, E. Manakova, A.
514 Ruksenaite, A. Silanskas, S. Asmontas, A. Grybauskas, U. Tylenyte, E. Jurgelaitis, R. Grigaitis, K. Timinskas, Č.
515 Venclovas, V. Siksnys, Short prokaryotic Argonautes provide defence against incoming mobile genetic elements
516 through NAD⁺ depletion, *Nat. Microbiol.* 2022. (2022) 1–13. <https://doi.org/10.1038/s41564-022-01239-0>.

517 [36] B. Koopal, A. Potocnik, S.K. Mutte, C. Aparicio-Maldonado, S. Lindhoud, J.J.M. Vervoort, S.J.J. Brouns, D.C. Swarts,
518 Short prokaryotic Argonaute systems trigger cell death upon detection of invading DNA, *Cell*. 185 (2022) 1471–
519 1486.e19. <https://doi.org/10.1016/j.cell.2022.03.012>.

520 [37] J. Garb, A. Lopatina, A. Bernheim, M. Zaremba, V. Siksnys, S. Melamed, A. Leavitt, A. Millman, G. Amitai, R. Sorek,
521 Multiple phage resistance systems inhibit infection via SIR2-dependent NAD⁺ depletion, *Nat. Microbiol.* 2022. (2022)
522 1–8. <https://doi.org/10.1038/s41564-022-01207-8>.

523 [38] S. Willkomm, K.S. Makarova, D. Grohmann, DNA silencing by prokaryotic Argonaute proteins adds a new layer of
524 defense against invading nucleic acids, *FEMS Microbiol. Rev.* 42 (2018) 376–387.
525 <https://doi.org/10.1093/femsre/fuy010>.

526 [39] A.M. Burroughs, L.M. Iyer, L. Aravind, Two novel PIWI families: Roles in inter-genomic conflicts in bacteria and
527 Mediator-dependent modulation of transcription in eukaryotes, *Biol. Direct.* 8 (2013) 1–15. [https://doi.org/10.1186/1745-6150-8-13](https://doi.org/10.1186/1745-
528 6150-8-13).

529 [40] S. Willkomm, C.A. Oellig, A. Zander, T. Restle, R. Keegan, D. Grohmann, S. Schneider, Structural and mechanistic
530 insights into an archaeal DNA-guided Argonaute protein, *Nat. Microbiol.* 2 (2017) 17035.
531 <https://doi.org/10.1038/nmicrobiol.2017.35>.

532 [41] P. Bryant, G. Pozzati, A. Elofsson, Improved prediction of protein-protein interactions using AlphaFold2, *Nat. Commun.*
533 13 (2022) 1–11. <https://doi.org/10.1038/s41467-022-28865-w>.

534 [42] S. Kim, Y. Jung, D. Lim, Argonaute system of *Kordia jejudonensis* is a heterodimeric nucleic acid-guided nuclease,
535 *Biochem. Biophys. Res. Commun.* 525 (2020) 755–758. <https://doi.org/10.1016/j.bbrc.2020.02.145>.

536 [43] E. Golovinas, D. Rutkauskas, E. Manakova, M. Jankunec, A. Silanskas, G. Sasnauskas, M. Zaremba, Prokaryotic
537 Argonaute from *Archaeoglobus fulgidus* interacts with DNA as a homodimer, *Sci. Rep.* 11 (2021) 1–14.
538 <https://doi.org/10.1038/s41598-021-83889-4>.

539 [44] A. Lopatina, N. Tal, R. Sorek, Abortive Infection: Bacterial Suicide as an Antiviral Immune Strategy, *Annu. Rev. Virol.* 7
540 (2020) 371–384. <https://doi.org/10.1146/annurev-virology-011620-040628>.

541 [45] S. Yeom, J. Oh, J.S. Lee, Spreading-dependent or independent Sir2-mediated gene silencing in budding yeast, *Genes*
542 and *Genomics*. 44 (2022) 359–367. <https://doi.org/10.1007/s13258-021-01203-y>.

543 [46] L. Onn, M. Portillo, S. Ilic, G. Cleitman, D. Stein, S. Kaluski, I. Shirat, Z. Slobodnik, M. Einav, F. Erdel, B. Akabayov, D.
544 Toiber, SIRT6 is a DNA double-strand break sensor, *Elife*. 9 (2020) 1–26. <https://doi.org/10.7554/elife.51636>.

545 [47] A. Vendrell, M. Martínez-Pastor, A. González-Novo, A. Pascual-Ahuir, D.A. Sinclair, M. Proft, F. Posas, Sir2 histone
546 deacetylase prevents programmed cell death caused by sustained activation of the Hog1 stress-activated protein
547 kinase, *EMBO Rep.* 12 (2011) 1062–1068. <https://doi.org/10.1038/embor.2011.154>.

548 [48] Q. Ma, T.K. Wood, Protein acetylation in prokaryotes increases stress resistance, *Biochem. Biophys. Res. Commun.*
549 410 (2011) 846–851. <https://doi.org/10.1016/j.bbrc.2011.06.076>.

550 [49] P. Mishra, S. Beura, S. Sikder, A.K. Dhal, M. Vasudevan, M. Roy, J. Rakshit, R. Budhwar, T.K. Kundu, R. Modak,
551 vp1524, a *Vibrio parahaemolyticus* NAD⁺-dependent deacetylase, regulates host response during infection by
552 induction of host histone deacetylation, *J. Biochem.* 171 (2022) 673–693. <https://doi.org/10.1093/jb/mvac027>.

553 [50] G. Ofir, E. Herbst, M. Baroz, D. Cohen, A. Millman, S. Doron, N. Tal, D.B.A. Malheiro, S. Malitsky, G. Amitai, R. Sorek,
554 Antiviral activity of bacterial TIR domains via immune signalling molecules, *Nature*. 600 (2021) 116–120.
555 <https://doi.org/10.1038/s41586-021-04098-7>.

556 [51] K.-Y. Yoda, H. Yasuda, X.-W. Jiang, T. Okazaki, RNA-primed initiation sites of DNA replication in the origin region of
557 bacteriophage lambda genome, *Nucleic Acids Res.* 16 (1988) 6531–6546.

558 [52] S. Doron, S. Melamed, G. Ofir, A. Leavitt, A. Lopatina, M. Keren, G. Amitai, R. Sorek, Systematic discovery of
559 antiphage defense systems in the microbial pan-genome, *Science*. 359 (2018) 0–12.
560 <https://doi.org/10.1126/science.aar4120>.

561 [53] T. Pawson, P. Nash, Assembly of cell regulatory systems through protein interaction domains, *Science*. 300 (2003)
562 445–452. <https://doi.org/10.1126/science.1083653>.

563 [54] K. Essuman, D.W. Summers, Y. Sasaki, X. Mao, A.K.Y. Yim, A. DiAntonio, J. Milbrandt, TIR Domain Proteins Are an
564 Ancient Family of NAD⁺-Consuming Enzymes, *Curr. Biol.* 28 (2018) 421–430.
565 <https://doi.org/10.1016/j.cub.2017.12.024>.

566 [55] K. Essuman, D.W. Summers, Y. Sasaki, X. Mao, A. DiAntonio, J. Milbrandt, The SARM1 Toll/Interleukin-1 Receptor
567 Domain Possesses Intrinsic NAD⁺ Cleavage Activity that Promotes Pathological Axonal Degeneration., *Neuron*. 93
568 (2017) 1334–1343. <https://doi.org/10.1016/j.neuron.2017.02.022>.

569 [56] E.L. Hopkins, W. Gu, B. Kobe, M.P. Coleman, A Novel NAD Signaling Mechanism in Axon Degeneration and its
570 Relationship to Innate Immunity, *Front. Mol. Biosci.* 8 (2021) 1–16. <https://doi.org/10.3389/fmabol.2021.703532>.

571 [57] S. Horsefield, H. Burdett, X. Zhang, M.K. Manik, Y. Shi, J. Chen, T. Qi, J. Gilley, J.-S. Lai, M.X. Rank, L.W. Casey, W.
572 Gu, D.J. Ericsson, G. Foley, R.O. Hughes, T. Bosanac, M. von Itzstein, J.P. Rathjen, J.D. Nanson, M. Boden, I.B. Dry,
573 S.J. Williams, B.J. Staskawicz, M.P. Coleman, T. Ve, P.N. Dodds, B. Kobe, NAD⁺ cleavage activity by animal and
574 plant TIR domains in cell death pathways, *Science*. 365 (2019) 793–799. <https://doi.org/10.1126/science.aax1911>.

575 [58] S.A. Killackey, M.A. Rahman, F. Soares, A.B. Zhang, M. Abdel-Nour, D.J. Philpott, S.E. Girardin, The mitochondrial
576 Nod-like receptor NLRX1 modifies apoptosis through SARM1, *Mol. Cell. Biochem.* 453 (2019) 187–196.

577 https://doi.org/10.1007/s11010-018-3444-3.

578 [59] L. Wan, K. Essuman, R.G. Anderson, Y. Sasaki, F. Monteiro, E.H. Chung, E.O. Nishimura, A. DiAntonio, J. Milbrandt, J.L. Dangl, M.T. Nishimura, TIR domains of plant immune receptors are NAD+-cleaving enzymes that promote cell death, *Science*. 365 (2019) 799–803. <https://doi.org/10.1126/science.aax1771>.

581 [60] Z. Duxbury, S. Wang, C.I. MacKenzie, J.L. Tenthorey, X. Zhang, S.U. Huh, L. Hu, L. Hill, P.M. Ngou, P. Ding, J. Chen, Y. Ma, H. Guo, B. Castel, P.N. Moschou, M. Bernoux, P.N. Dodds, R.E. Vance, J.D.G. Jones, Induced proximity of a TIR signaling domain on a plant-mammalian NLR chimera activates defense in plants, *Proc. Natl. Acad. Sci. U. S. A.* 117 (2020) 18832–18839. <https://doi.org/10.1073/pnas.2001185117>.

585 [61] B.R. Morehouse, A.A. Govande, A. Apurva, A. Millman, A.F. Keszei, B. Duncan-lowey, G. Ofir, S. Shao, R. Sorek, P.J. Kranzusch, STING cyclic dinucleotide sensing originated in bacteria, *Nature*. 586 (2020) 429–433. <https://doi.org/10.1038/s41586-020-2719-5>.

588 [62] N. Tal, B.B. Morehouse, A. Millman, A. Stokar-avihail, C. Avraham, T. Fedorenko, E. Yirmiya, E. Herbst, A. Brandis, T. Mehlman, A.F.A. Keszei, S. Shao, G. Amitai, P.J. Kranzusch, R. Sorek, Cyclic CMP and cyclic UMP mediate bacterial immunity against phages, *Cell*. 184 (2021) 5728-5739.e16. <https://doi.org/10.1016/j.cell.2021.09.031>.

591 [63] G. Hogrel, A. Guild, S. Graham, H. Rickman, S. Grüschow, Q. Bertrand, L. Spagnolo, M.F. White, Cyclic nucleotide-induced superhelical structure activates a bacterial TIR immune effector, *Nature*. 1 (2022) 2022.05.04.490601. <https://doi.org/10.1038/s41586-022-05070-9>.

594 [64] S. Eastman, T. Smith, M.A. Zayzman, P. Kim, S. Martinez, N. Damaraju, A. DiAntonio, J. Milbrandt, T.E. Clemente, J.R. Alfano, M. Guo, A phytobacterial TIR domain effector manipulates NAD+ to promote virulence, *New Phytol*. 233 (2022) 890–904. <https://doi.org/10.1111/nph.17805>.

597 [65] S. Ma, D. Lapin, L. Liu, Y. Sun, W. Song, X. Zhang, E. Logemann, Direct pathogen-induced assembly of an NLR immune receptor complex to form a holoenzyme, *Science*. 370 (2020). <https://doi.org/10.1126/science.abe3069>.

599 [66] R. Martin, T. Qi, H. Zhang, F. Liu, M. King, C. Toth, E. Nogales, B.J. Staskawicz, Structure of the activated ROQ1 600 resistosome directly recognizing the pathogen effector XopQ, *Science*. 370 (2020). <https://doi.org/10.1126/science.abd9993>.

602 [67] P.A. Waite-Rees, C.J. Keating, L.S. Moran, B.E. Slatko, L.J. Hornstra, J.S. Benner, Characterization and Expression of 603 the *Escherichia coli* Mrr Restriction System, *J. Bacteriol*. 173 (1991) 5207–5219.

604 [68] B. Lowey, A.T. Whiteley, A.F.A. Keszei, B.R. Morehouse, I.T. Mathews, S.P. Antine, V.J. Cabrera, D. Kashin, P. 605 Niemann, M. Jain, F. Schwede, J.J. Mekalanos, S. Shao, A.S.Y. Lee, P.J. Kranzusch, CBASS Immunity Uses CARF- 606 Related Effectors to Sense 3'-5'- and 2'-5'-Linked Cyclic Oligonucleotide Signals and Protect Bacteria from Phage 607 Infection, *Cell*. 182 (2020) 38-49.e17. <https://doi.org/10.1016/j.cell.2020.05.019>.

608 [69] A.J. Meeske, S. Nakandakari-Higa, L.A. Marraffini, Cas13-induced cellular dormancy prevents the rise of CRISPR- 609 resistant bacteriophage, *Nature*. 570 (2019) 241–245. <https://doi.org/10.1038/s41586-019-1257-5>.

610 [70] D. Mayo-Muñoz, L.M. Smith, C. Garcia-Doval, L.M. Malone, S.A. Jackson, H.G. Hampton, R.D. Fagerlund, P.C. 611 Fineran, Type III CRISPR-Cas provides resistance against nucleus-forming jumbo phages via abortive infection, 612 *BioRxiv*. (n.d.). <https://doi.org/10.1101/2022.06.20.496707>.

613 [71] J.E. Garneau, M.-E. V. Dupuis, M. Villion, D.A. Romero, R. Barrangou, P. Boyaval, C. Fremaux, P. Horvath, A.H. 614 Magadán, S. Moineau, The CRISPR/Cas bacterial immune system cleaves bacteriophage and plasmid DNA, (2010). 615 <https://doi.org/10.1038/nature09523>.

616 [72] B. Zetsche, J.S. Gootenberg, O.O. Abudayyeh, I.M. Slaymaker, K.S. Makarova, P. Essletzbichler, S.E. Volz, J. Joung,
617 J. Van Der Oost, A. Regev, E. V. Koonin, F. Zhang, Cpf1 Is a Single RNA-Guided Endonuclease of a Class 2 CRISPR-
618 Cas System, *Cell*. 163 (2015) 759–771. <https://doi.org/10.1016/j.cell.2015.09.038>.

619 [73] M. Jinek, K. Chylinski, I. Fonfara, M. Hauer, J.A. Doudna, E. Charpentier, A Programmable Dual-RNA-Guided DNA
620 Endonuclease in Adaptive Bacterial Immunity, *Science*. 337 (2012) 816–822. <https://doi.org/10.1126/science.1225829>.

621 [74] J.S. Parker, S.M. Roe, D. Barford, Crystal structure of a PIWI protein suggests mechanisms for siRNA recognition and
622 slicer activity, *EMBO J*. 23 (2004) 4727–4737. <https://doi.org/10.1038/sj.emboj.7600488>.

623 [75] J.-B. Ma, Y.-R. Yuan, G. Meister, Y. Pei, T. Tuschl, D.J. Patel, Structural basis for 5'-end-specific recognition of guide
624 RNA by the *A. fulgidus* Piwi protein, *Nature*. 434 (2005) 666–670. <https://doi.org/10.1038/nature03514>.

625 [76] R.W. Carthew, E.J. Sontheimer, Origins and Mechanisms of miRNAs and siRNAs, *Cell*. 136 (2009) 642–655.
626 <https://doi.org/10.1016/J.CELL.2009.01.035>.

627 [77] X. Liu, K. Fortin, Z. Mourelatos, MicroRNAs: Biogenesis and Molecular Functions, *Brain Pathol*. 18 (2008) 113–121.
628 <https://doi.org/10.1111/J.1750-3639.2007.00121.X>.

629 [78] M. Ha, V. Narry Kim, Regulation of microRNA biogenesis, (2014). <https://doi.org/10.1038/nrm3838>.

630 [79] I. Gainetdinov, C. Colpan, A. Arif, K. Cecchini, P.D. Zamore, A Single Mechanism of Biogenesis, Initiated and Directed
631 by PIWI Proteins, Explains piRNA Production in Most Animals, *Mol. Cell*. 71 (2018) 775–790.e5.
632 <https://doi.org/10.1016/J.MOLCEL.2018.08.007>.

633 [80] K.S. Makarova, Y.I. Wolf, J. Iranzo, S.A. Shmakov, O.S. Alkhnbashi, S.J.J. Brouns, E. Charpentier, D. Cheng, D.H.
634 Haft, P. Horvath, S. Moineau, F.J.M. Mojica, D. Scott, S.A. Shah, V. Siksny, M.P. Terns, Č. Venclovas, M.F. White,
635 A.F. Yakunin, W. Yan, F. Zhang, R.A. Garrett, R. Backofen, J. van der Oost, R. Barrangou, E. V. Koonin, Evolutionary
636 classification of CRISPR–Cas systems: a burst of class 2 and derived variants, *Nat. Rev. Microbiol.* (2019).
637 <https://doi.org/10.1038/s41579-019-0299-x>.

638 [81] F. Huang, X. Xu, H. Dong, N. Li, B. Zhong, H. Lu, Q. Liu, Y. Feng, Catalytic properties and biological function of a PIWI
639 - RE nuclease from *Pseudomonas stutzeri*, *Bioresour. Bioprocess.* (2022). <https://doi.org/10.1186/s40643-022-00539-x>.

641 [82] M. Jaskólska, D.W. Adams, M. Blokesch, Two defence systems eliminate plasmids from seventh pandemic *Vibrio*
642 *cholerae*, *Nature*. 14 (2022). <https://doi.org/10.1038/s41586-022-04546-y>.

643 [83] J.S. Chen, E. Ma, L.B. Harrington, M. Da Costa, X. Tian, J.M. Palefsky, J.A. Doudna, CRISPR-Cas12a target binding
644 unleashes indiscriminate single-stranded DNase activity, *Science*. 360 (2018) 436–439.
645 <https://doi.org/10.1126/science.aar6245>.

646 [84] J.S. Gootenberg, O.O. Abudayyeh, J.W. Lee, P. Essletzbichler, A.J. Dy, J. Joung, V. Verdine, N. Donghia, N.M.
647 Daringer, C.A. Freije, C. Myhrvold, R.P. Bhattacharyya, J. Livny, A. Regev, E. V Koonin, D.T. Hung, P.C. Sabeti, J.J.
648 Collins, F. Zhang, Nucleic acid detection with CRISPR-Cas13a/C2c2, *Science*. 356 (2017) 438–442.
649 <https://doi.org/10.1126/science.aam9321>.

650 [85] L. Li, S. Li, N. Wu, J. Wu, G. Wang, G. Zhao, J. Wang, HOLMESv2: A CRISPR-Cas12b-Assisted Platform for Nucleic
651 Acid Detection and DNA Methylation Quantitation, *ACS Synth. Biol.* 8 (2019) 2228–2237.
652 <https://doi.org/10.1021/acssynbio.9b00209>.

653 [86] J.A. Steens, Y. Zhu, D.W. Taylor, J.P.K. Bravo, S.H.P. Prinsen, C.D. Schoen, B.J.F. Keijser, M. Ossendrijver, L.M.

654 Hofstra, S.J.J. Brouns, A. Shinkai, J. van der Oost, R.H.J. Staals, SCOPE enables type III CRISPR-Cas diagnostics
655 using flexible targeting and stringent CARF ribonuclease activation, *Nat. Commun.* 12 (2021) 1–12.
656 <https://doi.org/10.1038/s41467-021-25337-5>.

657 [87] Y. Qin, Y. Li, Y. Hu, Emerging Argonaute-based nucleic acid biosensors, *Trends Biotechnol.* xx (2022) 4–8.
658 <https://doi.org/10.1016/j.tibtech.2022.03.006>.

659 [88] F. Frank, N. Sonenberg, B. Nagar, Structural basis for 5'-nucleotide base-specific recognition of guide RNA by human
660 AGO2, *Nature*. 465 (2010) 818–822. <https://doi.org/10.1038/nature09039>.

661 [89] M. Nowotny, S.A. Gaidamakov, R.J. Crouch, W. Yang, Crystal structures of RNase H bound to an RNA/DNA hybrid:
662 Substrate specificity and metal-dependent catalysis, *Cell*. 121 (2005) 1005–1016.
663 <https://doi.org/10.1016/j.cell.2005.04.024>.

664 [90] D.P. Bartel, MicroRNAs: Genomics, Biogenesis, Mechanism, and Function, *Cell*. 116 (2004) 281–297.
665 [https://doi.org/10.1016/S0092-8674\(04\)00045-5](https://doi.org/10.1016/S0092-8674(04)00045-5).

666 [91] K. Nakanishi, D.E. Weinberg, D.P. Bartel, D.J. Patel, Structure of yeast Argonaute with guide RNA, *Nature*. 486 (2012)
667 368–374. <https://doi.org/10.1038/nature11211>.

668 [92] J.S. Parker, How to slice: Snapshots of Argonaute in action, *Silence*. 1 (2010) 1–10. <https://doi.org/10.1186/1758-907X-1-3>.

670 [93] G.R. Chen, H. Sive, D.P. Bartel, A Seed Mismatch Enhances Argonaute2-Catalyzed Cleavage and Partially Rescues
671 Severely Impaired Cleavage Found in Fish, *Mol. Cell*. 68 (2017) 1095–1107.e5.
672 <https://doi.org/10.1016/j.molcel.2017.11.032>.

673 [94] J. Sheu-Gruttaduria, P. Pawlica, S.M. Klum, S. Wang, T.A. Yario, N.T. Schirle Oakdale, J.A. Steitz, I.J. MacRae,
674 Structural Basis for Target-Directed MicroRNA Degradation, *Mol. Cell*. 75 (2019) 1243–1255.e7.
675 <https://doi.org/10.1016/j.molcel.2019.06.019>.

676 [95] A. Kuzmenko, D. Yudin, S. Ryazansky, A. Kulbachinskiy, A. Aravin, Programmable DNA cleavage by Ago nucleases
677 from mesophilic bacteria *Clostridium butyricum* and *Limnothrix rosea*, *BioRxiv*. (2019) 558684.
678 <https://doi.org/10.1101/558684>.

679 [96] P.B. Kwak, Y. Tomari, The N domain of Argonaute drives duplex unwinding during RISC assembly, *Nat. Struct. Mol.*
680 *Biol.* 19 (2012) 145–151. <https://doi.org/10.1038/nsmb.2232>.

681 [97] T. Kawamata, H. Seitz, Y. Tomari, Structural determinants of miRNAs for RISC loading and slicer-independent
682 unwinding, *Nat. Struct. Mol. Biol.* 16 (2009) 953–960. <https://doi.org/10.1038/nsmb.1630>.

683 [98] Y. Tian, D.K. Simanshu, J.B. Ma, D.J. Patel, Structural basis for piRNA 2'-O-methylated 3'-end recognition by Piwi PAZ
684 (Piwi/Argonaute/Zwille) domains, *Proc. Natl. Acad. Sci. U. S. A.* 108 (2011) 903–910.
685 <https://doi.org/10.1073/pnas.1017762108>.

686 [99] Y. Wang, S. Juranek, H. Li, G. Sheng, G.S. Wardle, T. Tuschl, D.J. Patel, Nucleation, propagation and cleavage of
687 target RNAs in Ago silencing complexes, *Nature*. 461 (2009) 754–761. <https://doi.org/10.1038/nature08434>.

688 [100] G. Meister, L. Jakob, K. Kramm, V. Graus, J. Neumeier, D. Grohmann, Single-molecule FRET uncovers hidden
689 conformations and dynamics of human Argonaute 2, (2022) 1–13. <https://doi.org/10.1038/s41467-022-31480-4>.

690 [101] Y. Liu, D. Esyunina, I. Olovnikov, M. Teplova, A. Kulbachinskiy, A.A. Aravin, D.J. Patel, Accommodation of Helical
691 Imperfections in *Rhodobacter sphaeroides* Argonaute Ternary Complexes with Guide RNA and Target DNA, *Cell Rep.*

692 24 (2018) 453–462. <https://doi.org/10.1016/j.celrep.2018.06.021>.

693 [102] T. Miyoshi, K. Ito, R. Murakami, T. Uchiumi, Structural basis for the recognition of guide RNA and target DNA
694 heteroduplex by Argonaute, *Nat. Commun.* 7 (2016) 1–12. <https://doi.org/10.1038/ncomms11846>.

695 [103] L. Holm, Dali server: structural unification of protein families, *Nucleic Acids Res.* 50 (2022).
696 <https://doi.org/10.1093/nar/gkac387>.

697